

Research paper

Adaptive hydraulic strategies of *Pinus tabuliformis* to drought across moisture-level slopes in the central Qinling Mountains, ChinaLingnan Zhang^a, Yixue Hong^b, Yanjun Song^c, Xiaohong Liu^{a,d,*}, Xiaomin Zeng^a, Yan Liu^a, Gonzalo Pérez-de-Lis^e^a School of Geography and Tourism, Shaanxi Normal University, Xi'an 710119, China^b State Key Laboratory of Biocontrol, School of Ecology, Shenzhen Campus of Sun Yat-Sen University, Shenzhen 518107, China^c School of Biological Sciences, Washington State University, Pullman, WA 99163, USA^d Shaanxi Observation and Research Station for Ecology and Environment of Desert-Loess Zone at Yulin, Xi'an 710119, China^e BIOAPLIC, Departamento de Botánica, Universidade de Santiago de Compostela, EPSE, Campus Terra, Lugo 27002, Spain

ARTICLE INFO

Keywords:

Drought
Intrinsic water-use efficiency
Pinus tabuliformis
Tree rings
Wood anatomy

ABSTRACT

Understanding the response mechanism of tree growth to climate change is essential for predicting future forest dynamics in temperate regions facing significant warming and drying situations. However, the mechanisms by which trees adjust their hydraulic structure, growth and physiology in response to water stress and their effects on radial growth and canopy dynamics across different moisture environments remain poorly understood. We investigate the strategies employed by *Pinus tabuliformis* on dry and wet slopes of the central Qinling Mountains in China to adapt their xylem to climate variability, using anatomical indicators (theoretical hydraulic conductivity (Kh), cell wall thickness, and conduit wall reinforcement (CWR)), tree-ring width and intrinsic water-use efficiency (iWUE) derived from $\delta^{13}\text{C}$ analyses. Contrasting drought adjustment strategies were observed on dry and wet slopes. Trees on the drier slope deployed a relatively acquisitive strategy characterized by higher Kh and lower CWR. In contrast, trees on wetter slopes adopted a relatively conservative strategy with lower Kh and higher CWR. Under increasing drought severity, trees demonstrated a rise in iWUE, which has the potential to strengthen the response of hydraulic efficiency and safety indicators to precipitation. Moreover, anatomical structure and iWUE differentially affected tree-ring width and Enhanced Vegetation Index at various growing stages. Increasing iWUE could not prevent a decline in radial growth under unfavorable moisture conditions. These findings offer foundational insights into the physiological mechanisms used by *P. tabuliformis* to adapt to environmental changes in temperate areas, highlighting the complex interactions among climate, anatomical and physiological indicators, and growth dynamics.

1. Introduction

Global climate change, an indisputable reality, is projected to persist throughout the coming century (IPCC, 2021). Slow xylem growth in trees hinders their rapid adaptation to environmental shifts, making them vulnerable to rapid climate change (Brodrribb et al., 2020). Increased warming, coupled with reduced global precipitation patterns, is expected to cause more frequent and intense droughts (Ault, 2020). Escalating droughts resulting from water deficits are contributing to forest degradation and mortality (Allen et al., 2010; Babst et al., 2019). This phenomenon is evident through a decline in tree growth, indicated by reduced tree-ring width and weakened canopy vegetation greenness

(Shi et al., 2024). These effects are not confined to arid regions, as they also appear in humid areas, which are generally considered less susceptible to drought (González-M et al., 2021). Therefore, understanding the adaptive strategies deployed by temperate trees to cope with climate variability and their effect on radial growth and canopy dynamics across different moisture levels is crucial for predicting forest development trends and forest carbon sequestration capacity in the face of climate change.

The xylem, a specialized vascular tissue, is essential for water and mineral transport and provides crucial mechanical support for plant growth (Růžička et al., 2015). In conifers, xylem is mainly formed by tracheids and parenchyma cells (Song et al., 2021). Tracheids are the

* Correspondence to: School of Geography and Tourism, Shaanxi Normal University, West Chang'an Street 620, Xi'an, Shaanxi 710119, China.
E-mail address: xhliu@snnu.edu.cn (X. Liu).

primary conductive cells. As reflected by various anatomical and functional traits, tracheid structure significantly influences the functional properties of xylem (Arguelles-Marron et al., 2023). For instance, a large lumen diameter (LD) enhances hydraulic efficiency, as indicated by an increase in hydraulic diameter (Dh) and theoretical hydraulic conductivity (Kh). Conversely, a large cell wall thickness (CWT) and reduced LD promote conduit wall reinforcement (CWR), which is associated with higher hydraulic safety (Lachenbruch and McCulloh, 2014; Schuldt et al., 2016). In response to water stress, trees modulate their tracheid structure, adopting strategies that balance hydraulic safety and efficiency. These strategies are categorized as conservative or acquisitive. In conservative adjustments, limited LD and large CWT minimize the risk of embolisms—air bubbles obstructing water flow through the xylem—at the cost of reducing hydraulic efficiency (Liang et al., 2013; Olano et al., 2014). On the contrary, acquisitive adjustments (large LD and reduced CWT) may allow a greater water flow to the leaves for photosynthesis at the cost of increasing xylem vulnerability to cavitation (Eilmann et al., 2009; Martin-Benito et al., 2017; Tyree and Dixon, 1986). Studies on *Castanopsis fargesii* in subtropical China (Liang et al., 2019) and Eucalyptus species in Australia indicate that decreasing precipitation and increased drought intensity lead to reduced Kh, with species adapting by sacrificing hydraulic efficiency for hydraulic safety (Pfausch et al., 2016). In northeast China, *P. tabuliformis* adjusts its strategy, favoring hydraulic safety in dry conditions but hydraulic efficiency in wet conditions in response to drought and warming (Song et al., 2022). It can be inferred that many species tend to employ aggressive strategies in well-watered environments and conservative strategies in water-limited conditions.

Besides xylem anatomy, the stable carbon isotope ratio ($\delta^{13}\text{C}$) in tree rings also reflects trees' responses to climate. Under drought, trees adjust stomatal conductance and photosynthetic rates, altering isotope fractionation during CO_2 uptake and fixation in the leaves. These adjustments affect the $\delta^{13}\text{C}$ of the compounds used to build xylem cell walls (Granda et al., 2014; Saurer et al., 2004). The $\delta^{13}\text{C}$ is known to be a proxy of the intrinsic water-use efficiency (iWUE), which is the ratio of assimilation to stomatal conductance (Saurer and Voelker, 2022). An increase in iWUE indicates enhanced photosynthesis caused by increasing atmospheric CO_2 concentration and/or reduced transpiration owing to decreased stomatal conductance under dry conditions ((González de Andrés et al., 2021; Zuidema et al., 2020). However, those increases in iWUE usually can't translated into tree growth increment (Peñuelas et al., 2011). Therefore, when trees experience drought, they typically show a decrease in growth while exhibiting an increase in iWUE (Li et al., 2023; Wang et al., 2012).

Previous studies in conifers have examined the alterations in the xylem anatomy and iWUE in response to climate (Linares and Camarero, 2011; Puchi et al., 2021). However, the interconnection between these two aspects has received less attention (Castagneri et al., 2018; Puchi et al., 2021). In this regard, it would be worth investigating whether changes in iWUE influences the dynamic response of anatomical structures to climate.

The dynamics of radial growth and canopy development are thought to be modulated by xylem anatomy and iWUE. Lower hydraulic conductivity and higher hydraulic safety could reduce available water for trees and are thought to be unfavorable to tree radial growth and canopy development (Jia et al., 2022). For example, a study about *Pinus sylvestris* var. *Mongolica* found extreme drought event reduced xylem theoretical hydraulic conductivity and increased hydraulic safety, resulting in trunk radial increment stagnation in northern China (Han et al., 2023). High iWUE induced by drought is often observed to coincide with decreased radial growth in conifers (Chen et al., 2022; Zhang et al., 2023). However, the combined effect of xylem conduit adjustment and water use strategy on radial growth and canopy development remains largely obscured. A better understanding of the effect of xylem anatomy and iWUE on tree ring width and vegetation greenness would provide a more accurate basis for the evaluation of tree

performance and forest functioning.

This study aims to use functional traits derived from wood anatomy and $\delta^{13}\text{C}$ in *Pinus tabuliformis* Carr. growing on dry and humid slopes in the Qinling Mountains, which mark the boundary between northern and southern China and between temperate and subtropical monsoon climates. Predictive models suggest a significant temperature increase in this region over the next century (Wang and Chen, 2014; Zhang et al., 2013). This may provide an opportunity to investigate trees' strategies to adapt to climate change, as well as the potential interrelationships between these anatomical and functional traits. Additionally, we aim to assess their effects on tree growth, as indicated by the tree ring width index and canopy dynamics reflected by the Enhanced Vegetation Index (EVI). Our hypotheses are as follows: (1) *P. tabuliformis* show a conservative/acquisitive hydraulic adjustment to drought on the drier/wetter slope, exhibiting higher iWUE at the same time; (2) iWUE changes strengthens the response of anatomical indicators to climate; and (3) hydraulic safety and iWUE are negatively associated to radial growth and canopy development.

2. Materials and methods

2.1. Study area and climate

The Qinling Mountains serve as a crucial biogeographical boundary in China, separating the northern and southern regions and acting as a climatic threshold between subtropical and warm temperate zones. This intersection creates a unique transitional climate and a highly sensitive ecology. *Pinus tabuliformis*, a prevalent coniferous species, is widespread across the Qinling Mountains range. The Nanwutai National Forest Park (NWT; 108°57'–108°59' E, 33°58'–34°02' N), situated on the northern slope of the central Qinling Mountains, has a temperate continental monsoon climate and supports diverse vegetation types. Conversely, the Muwang National Forest Park (MW; 108°35'–108°42' E, 33°21'–33°28' N), located on the southern slope (Fig. 1), experiences a northern subtropical monsoon climate.

Climate data were got from the nearest meteorological stations—Chang'an (34°03' N, 108°31' E) for NWT and Zhen'an (33°15' N, 109°05' E) for MW (details in Fig. S1). The climate at NWT is generally drier than that at MW according to the mean precipitation minus potential evapotranspiration (P-PET) during 1960–2018 (Fig. 2). Both sites showed an upward trend in the mean maximum temperature (Tmax) throughout the year and during the growing season over the past six decades. However, P-PET has declined, indicating an increased aridity and warming (Fig. S2, Method S4).

2.2. Sampling and site chronology development

In August 2019, 73 and 72 thin tree-ring cores were collected from 36 healthy *P. tabuliformis* trees (diameter at breast height > 5.6 cm) at NWT and MW, respectively (details in Table S1). Tree-ring widths were measured using a Lintab 6.0 device (Rinn) and then the COFECHA program (Holmes, 1983) was used to verify the accuracy of the cross-dating and measurement process. The age trends of raw tree-ring width series were detrended using a cubic spline and the “dplr” package in R software to create standardized chronologies for the site and individual cores.

2.3. Establishing chronologies of earlywood and latewood width and anatomical indicators

Correlation coefficients were calculated between the chronology of each core and the site chronology to identify cores with a high correlation to site chronology. Anatomical experiments were then conducted on seven cores from NWT and six cores from MW, which exhibited strong correlations with the site chronology (Details in Method S1). Each ring was categorized as earlywood or latewood following Mork's index

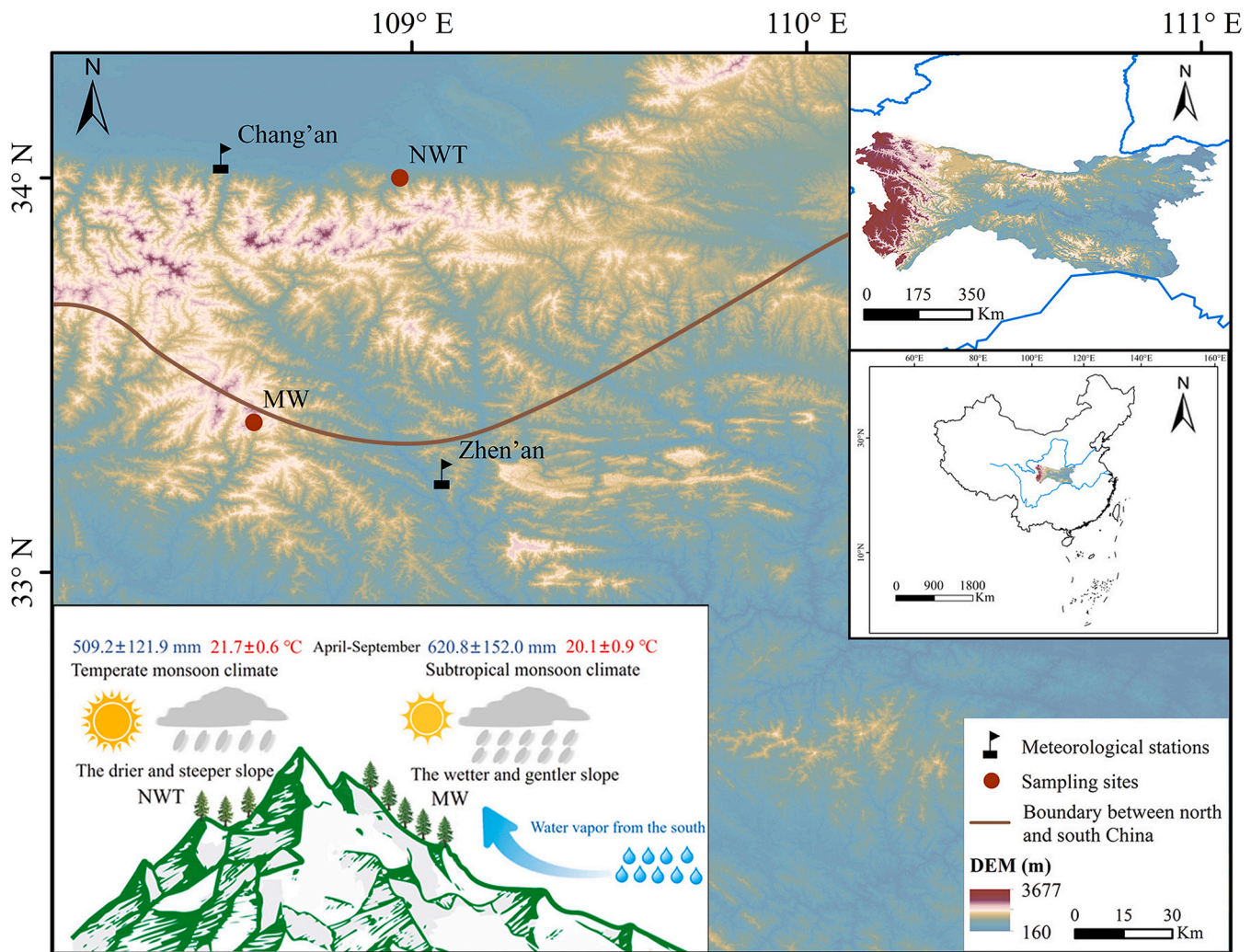


Fig. 1. The environments of sampling sites and the nearest weather stations in the central Qinling Mountains. Pre indicates total precipitation from April to September, Tmax indicates mean maximum temperature from April to September.

(Denne, 1989), and earlywood or latewood width series were then obtained. The mean LD and CWT were calculated annually for earlywood or latewood. Theoretical hydraulic efficiency indicators, Dh and Kh, were calculated as Method S2. All original anatomical series were also detrended using a cubic spline function to remove age-related effects. Bi-weight site chronologies for the tree-ring width series (earlywood or latewood) and 10 anatomical indicators were established using the R package “dplr” (Bunn, 2008), covering the years 1960–2018 (Table S2).

2.4. Intrinsic water-use efficiency assessed through carbon isotope in tree rings

Thick cores, equal in number to the thin cores used for anatomical analysis, were used to determine the $^{13}\text{C}/^{12}\text{C}$ isotope ratios in wood cellulose for the period 1960–2018. Details for measuring $\delta^{13}\text{C}$ and calculating iWUE are shown in Method S3. Ultimately, four physiological indicators were derived from the analysis, encompassing the $\delta^{13}\text{C}$ and iWUE for earlywood or latewood. In total, we obtained 16 anatomical and physiological indicators (Fig. 3, Table S2).

2.5. Analyzing statistics

Generalized Additive Models (GAMs), recognized as semi-parametric regression models, were employed to analyze low-frequency dynamics of tree-ring width and P-PET over various monthly combinations

(Method S4). Daily total precipitation (dPre) and daily mean maximum temperature (dTmax) were aggregated using 31-day moving windows from April 1 to September 30, spanning the period 1960–2018. Pearson’s correlation coefficients assessed the relationships between the first-order differences of dPre and dTmax with 16 anatomical and physiological indicators (Table S2). Pearson’s correlation analysis revealed that LD, Dh, and Kh exhibited analogous correlations with climate factors, while $\delta^{13}\text{C}$ and iWUE also showed similar correlations with climate factors (Fig. S3, Method S5). Therefore, we mainly focused on the research about 8 key radial indicators, including tree-ring width indices, two theoretical hydraulic indicators (i.e. Kh and CWR) and iWUE in earlywood or latewood (Fig. 4, Method S6), in the following analysis. To explore the potential effects of iWUE changes on the dynamic responses of Kh and CWR to climate, the relationships between 20-year moving mean values of iWUE and 20-year moving correlation coefficients mentioned above were analyzed by using GAMs for the period 1960–2018 (Method S7).

To assess variations in theoretical hydraulic indicators and iWUE under extreme wet and dry conditions, deviation values were calculated by comparing these indicators of latewood in extreme years and indicators of earlywood in the next years with the average values from 1960 to 2018. Z-score normalization was applied to the iWUE series of earlywood or latewood. Previous Pearson correlation analysis revealed that climate conditions from June to July significantly influenced anatomical and physiological indicators at the NWT site, while the

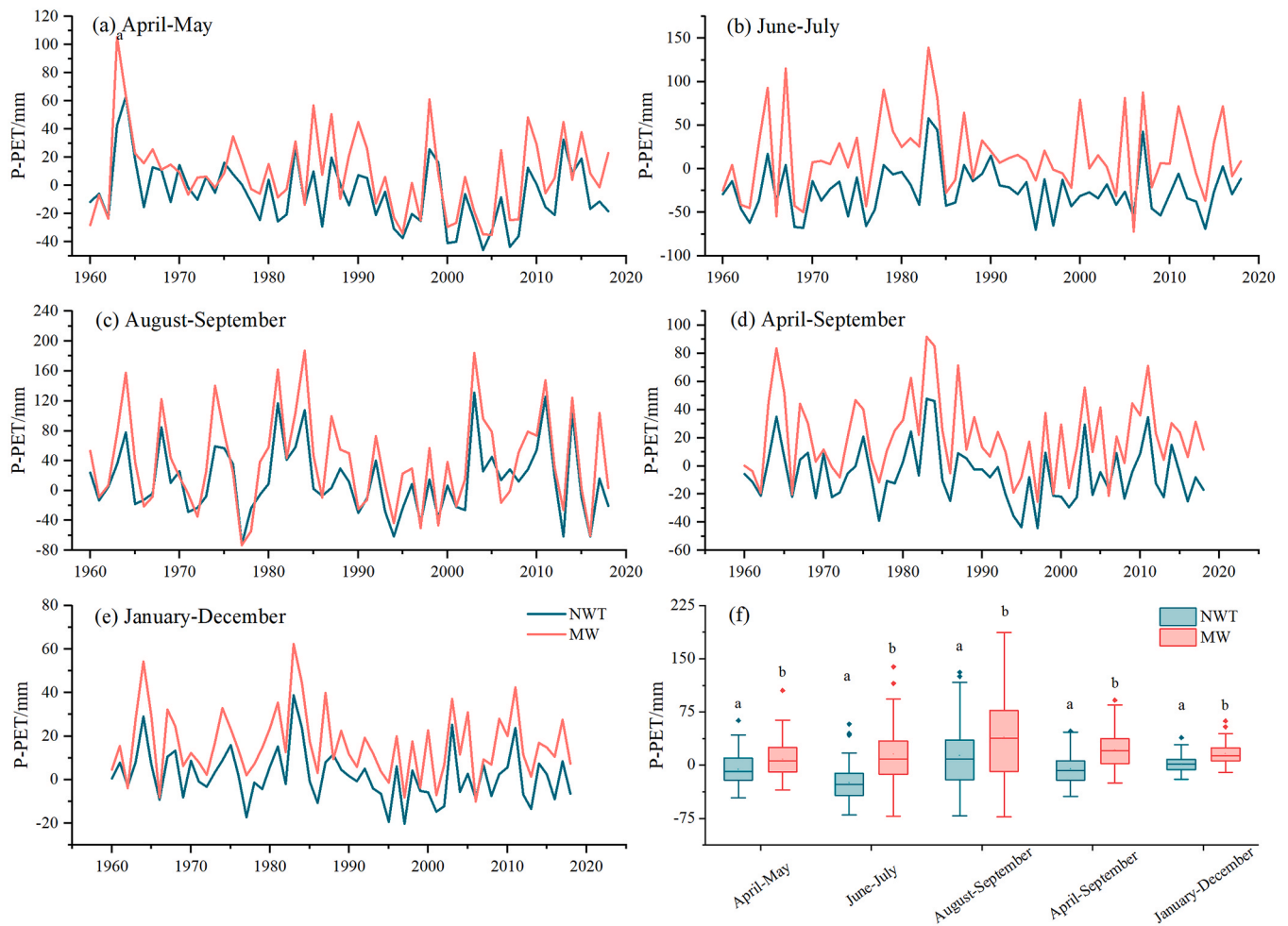


Fig. 2. Water balance indicated by mean precipitation minus potential evapotranspiration (P-PET) from different combinations of months during 1960–2018 (a-e). The significance of differences in water balance between the NWT site and the MW site was assessed by *t*-test (f).

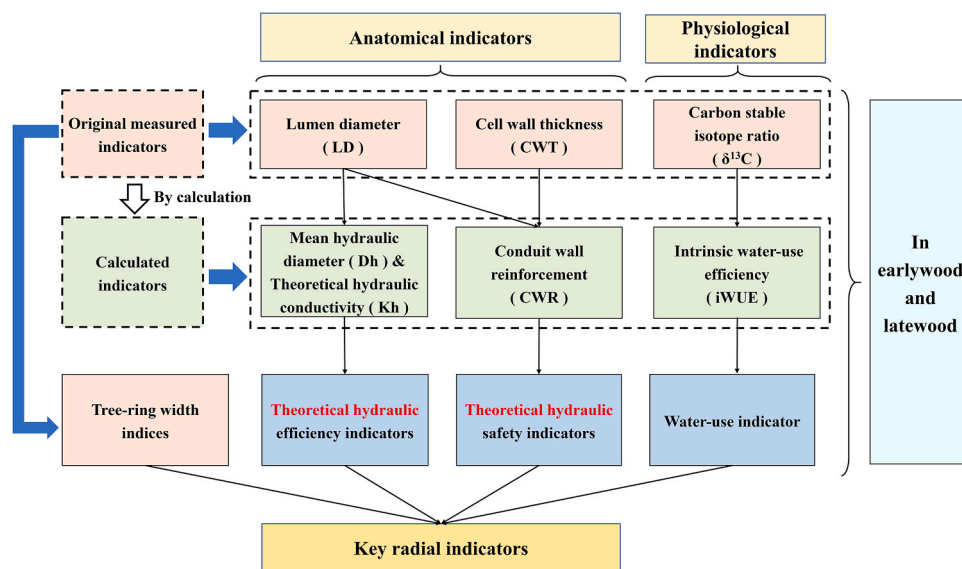


Fig. 3. Relationships among all indicators.

climate conditions from August to September had a substantial effect on the MW site (Fig. S3). Consequently, 1983 and 1995 were identified as extremely wet and dry years, respectively, for NWT based on the P-PET

from June to July. Similarly, for MW, 2003 and 1997 were selected as extremely wet and dry years, respectively, based on P-PET from August to September (Fig. 2). Furthermore, we validated the accuracy of the

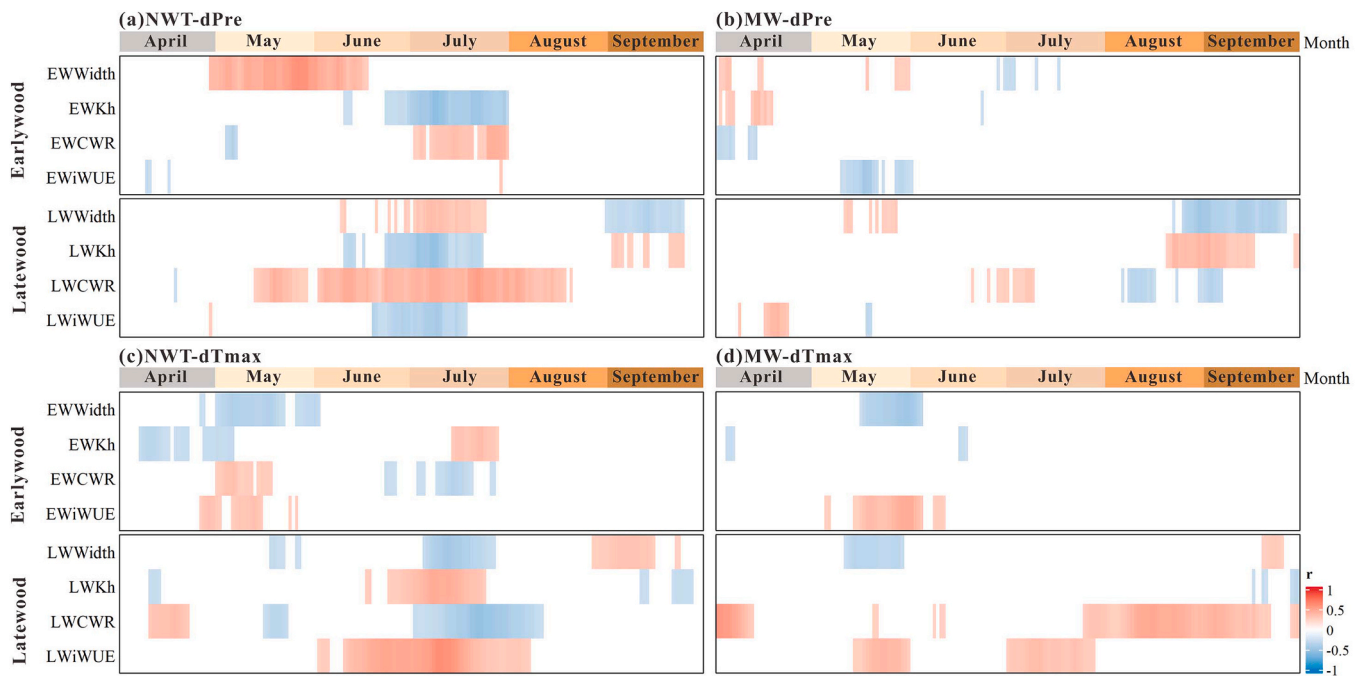


Fig. 4. Pearson's correlation coefficients (r) between first order difference series (fd) of daily total precipitation (dPre) and fd of 8 key radial indicators (a & b) and those between fd of the daily mean maximum temperature (dTmax) and fd of 8 key radial indicators (c & d) during 1960–2018 at NWT and MW. dPre and dTmax were calculated using 31-day moving windows from April 1 to September 30. The meanings of all abbreviations are displayed in Table S2.

year selections through a 2D kernel density analysis of Tmax and Pre during these periods (Fig. S4, Method S8).

Pearson's correlation was used to elucidate the correspondence of Kh, CWR, CWT of earlywood and iWUE of latewood to tree-ring width indices of latewood based on the first-order differences of these series. Seasonal and long-term canopy changes in *P. tabuliformis* were evaluated by analyzing a monthly time series of the Enhanced Vegetation Index (EVI) from 2000 to 2018. According to one research on xylogenesis of *P. tabuliformis* (data haven't been published), we assumed that EVI from June to early August corresponded to the earlywood formation period, while the EVI from late August to September corresponded to the latewood formation period. The EVI data, derived from the MOD13Q1 v006 product at a 250-m spatial resolution, were sourced from the NASA Earthdata portal (<https://earthdata.nasa.gov/>). Subsequently, GAMS were used to reflect the variations of anatomical indicators, iWUE, and EVI and the relationships among them (Method S9).

3. Results

3.1. Diverse responses of key radial indicators to long-term climate on two slopes with different moisture level

On a low-frequency scale, earlywood width was synchronized with the P-PET on both slopes during their respective critical periods (May to July for NWT and April to July for MW) (Fig. S5a and S5c), being also the case of latewood width in September (Fig. S5b and S5d). At the high-frequency scale, the relationships between tree-ring width indices and daily climate variables were more complex. At NWT, earlywood width exhibited positive correlations with dPre from May to mid-June and negative correlations with dTmax in May. The latewood width at NWT showed a positive correlation with dPre and a negative correlation with dTmax in July. At MW, earlywood width had a negative correlation with dTmax from mid-May to early June. Latewood width at both sites exhibited a negative correlation with dPre and a positive correlation with dTmax in the late growing season (Fig. 4).

Theoretical hydraulic indicators demonstrated sensitivity to inter-annual high-frequency climate variations (Fig. 4). At NWT, Kh of both

earlywood and latewood were negatively correlated with dPre and positively correlated with dTmax in the middle growing season. The earlywood CWR was positively correlated with dPre in July and dTmax in early to mid-May but negatively correlated with dTmax in July. In contrast, latewood CWR was positively correlated with dPre during the early to mid-growing seasons and negatively correlated with dTmax from July to early August. At the MW site, latewood Kh exhibited a positive correlation with dPre from late August to mid-September and a negative correlation with dTmax in late-September. The latewood CWR there was negatively correlated with dPre and positively correlated with dTmax during the late growing season.

High sensitivity to climate variation was also observed for iWUE, with earlywood iWUE at NWT being positively correlated with dTmax in early-mid May, and latewood iWUE being negatively correlated with dPre and positively correlated with dTmax from June to July (Fig. 4a and c). At MW, earlywood iWUE also displayed positive correlations with dTmax from mid-May to early June but negative correlations with dPre in May, whereas latewood iWUE showed positive correlations with dTmax in May and July (Fig. 4b and d).

3.2. Contrasting variations of theoretical hydraulic indicators and iWUE during extreme wet and dry years

At NWT, Kh and iWUE of latewood, and earlywood iWUE in the next year were lower in 1983 (extremely wet year) compared to their 1960–2018 averages, whereas higher-than-average values were found in 1995 (extremely dry year). In contrast, latewood CWR and earlywood CWR in the next year were comparatively higher in 1983, but lower in 1995 than its 1960–2018 average value (Fig. 5a). However, opposite results were found for these indicators at MW. Kh and iWUE of latewood, and earlywood iWUE in the next year were higher in 2003 (extremely wet year) but lower in 1977 (extremely dry year) compared to their 1960–2018 averages. Latewood CWR values were lower (higher) in 2003 (1977) than their respective mean values (Fig. 5b).

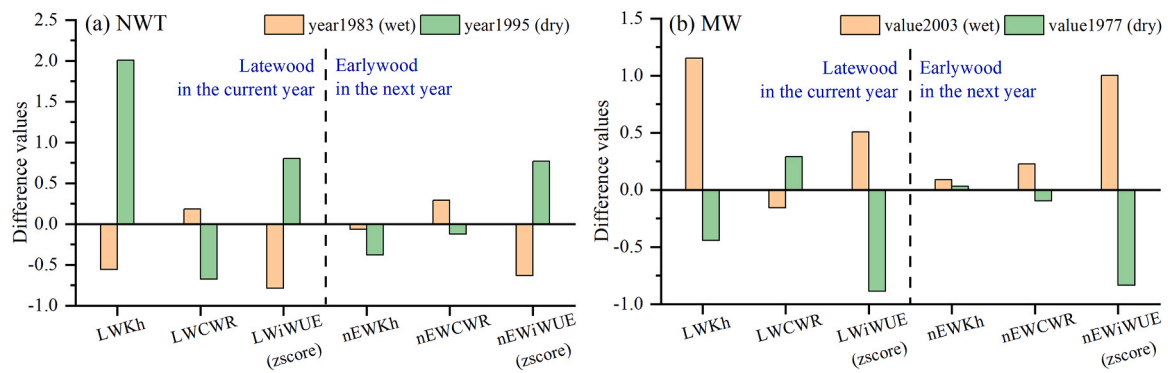


Fig. 5. Differences between anatomical and physiological indicators for an extremely wet and extremely dry year, and their mean values during 1960–2018 at NWT (a) and MW (b). EW indicates earlywood and LW indicates latewood. n indicates the corresponding next years.

3.3. Relationships between iWUE changes and dynamic responses of theoretical hydraulic indicators to climate

GAMs revealed that iWUE influenced the response of anatomical indicators to climatic factors. As earlywood iWUE increased at NWT, the negative response of earlywood Kh and positive response of earlywood CWR to total precipitation in July strengthened (Fig. 6a and b). Similarly, as latewood iWUE increased at NWT, the negative response of latewood Kh and positive response of latewood CWR to total precipitation in June–July strengthened when latewood iWUE was $< 145 \mu\text{mol mol}^{-1}$ (Fig. 6c and d). In contrast, as latewood iWUE increased at MW, the positive/negative response of latewood Kh/CWR to total precipitation in August–September strengthened on that slope (Fig. 6e and f).

3.4. Relationships between anatomical indicators and iWUE and tree-ring width and EVI

Pearson's correlation coefficients reflected the relationships between earlywood xylem anatomy latewood radial growth and latewood iWUE and latewood radial growth. Both at NWT and MW, lower CWT in earlywood sectors corresponded to the formation of narrower latewood sectors, while Kh in earlywood sectors didn't show significant relationships with latewood sectors. The narrower latewood sectors were a consequence of lower CWR in earlywood at MW. Additionally, the narrower the latewood sectors, the larger their corresponding iWUE values at the two sites (Fig. 7).

Both at NWT and MW, EVI during the earlywood (June to early August) and latewood (late August to September) formation periods increased from 2003 to 2015, which seemed to be affected the corresponding increasing iWUE with a time lag. Higher earlywood CWR corresponded with lower EVI values from late August to September. Similarly, higher EVI values from June to early August corresponded with lower earlywood CWT at the two sites. The correspondences between EVI values from late August to September and latewood CWT were positive at the drier slopes, but unstable at the wetter slopes (Fig. 8 and Fig. S6).

4. Discussion

4.1. Moisture-dependent strategies in the anatomical and physiological response of trees to climate

Long-term, low-frequency changes in earlywood and latewood widths after removing age trends were primarily influenced by water balance, as indicated by P-PET during the early to mid (earlywood) and late (latewood) growing season. On the drier slope (NWT), earlywood width varied positively with precipitation and negatively with mean maximum temperatures from May to early June, while latewood width showed similar correlations with those in precipitation and mean

maximum temperatures in July. On the wetter slope (MW), earlywood and latewood widths varied also negatively with the mean maximum temperature in mid to late May. These results suggest that early to mid-summer drought appears to be a major driver for changes in xylem cell production in our study pines, which agrees with previous studies in temperate and Mediterranean conifers (Castagneri et al., 2018). However, in the late growing season, latewood width varied positively with maximum temperature and negatively with precipitation, which could be related to a delayed cessation of xylem formation. These findings highlight the multiscale influence of climate on tree-ring width.

Contrary to our first hypothesis, *P. tabuliformis* show an acquisitive hydraulic adjustment and a conservative adjustment to drought on the drier and wetter slope, respectively, as suggested by the correlative analysis as well as by the differences in extremely wet and dry years compared to their 1960–2018 averages. On the wetter slope, latewood Kh varied positively with precipitation and negatively with maximum temperature in the late growing season, while latewood CWR responded positively to maximum temperature. Higher water availability on this slope may have fostered cell lumen enlargement through increased turgor pressure and primary cell wall pliability (Cosgrove, 2005; Hölttä et al., 2010). This is supported by the strong increase in latewood Kh observed in 2003 (extremely wet year). While high hydraulic conductivity may increase carbon assimilation rates under non-limiting water conditions, low Kh and high CWR may improve resistance to cavitation under drought (Hacke et al., 2001). Therefore, the observed decreasing latewood Kh and increasing latewood CWR in dry and warm August–September suggests that study pines adopted a conservative hydraulic strategy to enhance hydraulic safety to cope with warmer and drier conditions at the wetter site. Our results are in agreement with decreasing latewood Kh and increasing latewood CWR reported in *P. pinea* in response to a dry conditions in autumn (Castagneri et al., 2018). Similar strategies were observed in *Picea glauca* and *P. mariana* across the northern treeline in Canada, with narrower cells with thicker walls being produced under warm and dry summer conditions (Lange et al., 2020).

On the drier slope, however, Kh varied negatively with early-middle summer precipitation and positively with mid-summer mean maximum temperature, while CWR varied positively with precipitation, and negatively with mid-summer mean maximum temperature. These results suggest an acquisitive strategy to adapt to warm and dry conditions, where trees enhance their hydraulic efficiency by increasing Kh and reducing CWR. Although large average LD values under drought would be somewhat explained by a limited latewood production (Fernandez-de-Una et al., 2017), a previous study performed in central Spain noted that *P. nigra* and *P. sylvestris* form wider tracheid lumens and narrower walls as a response to drought (Martin-Benito et al., 2017). Similarly, it has been reported that *P. sylvestris* increases conduit diameter and reduces the carbon cost per tracheid to manage drought conditions in the alpine valleys of central Europe (Eilmann et al., 2009).

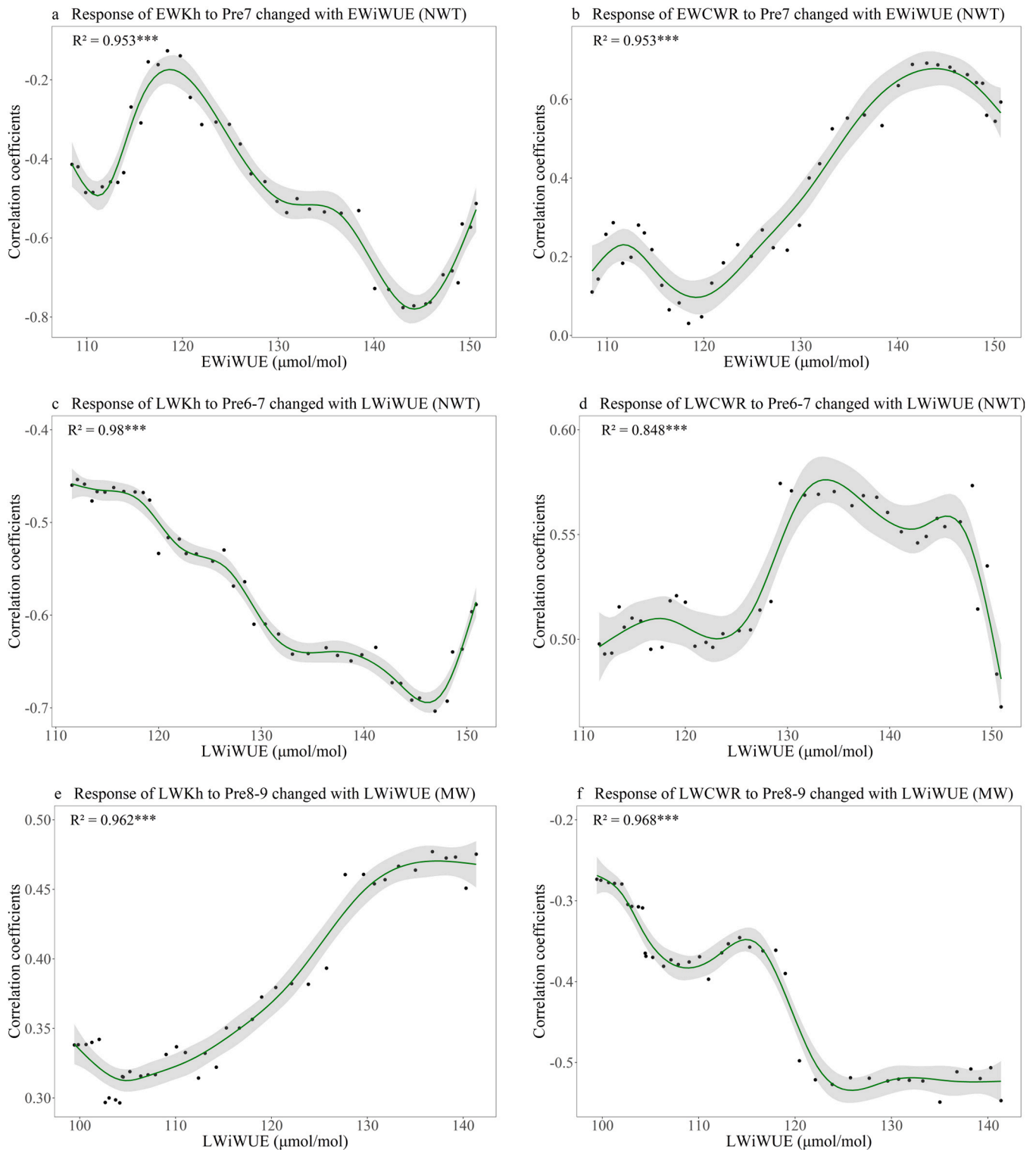


Fig. 6. Variation in 20-year moving correlation coefficients between theoretical hydraulic indicators (Kh and CWR) and precipitation, along with average iWUE for the corresponding 20 years at NWT (a–d) and MW (e, f) reflected by generalized additive model for the period 1960–2018. Pre7 indicates total precipitation in July, Pre6–7 indicates total precipitation in June–July, Pre8–9 indicates total precipitation in August–September. * * * indicates $P < 0.001$. EW indicates earlywood and LW indicates latewood.

Reduced CWR and narrower earlywood and latewood under drought could be both part of a strategy to prioritize carbon storage by limiting investment on cell wall construction and minimize the role of xylem as a carbon sink in periods of low assimilation (Olano et al., 2014; Piper et al., 2017). This would be reflected by the strong warming-induced increase in iWUE noted on the drier slope, which may be linked to

reductions in stomatal conductance, hence reducing water loss and CO_2 acquisition, rather than to higher photosynthetic rates (Brodribb and McAdam, 2017; Linares and Camarero, 2011; Sperry et al., 2017).

Study pines on both slopes exhibited similar physiological adjustments to climate variability, increasing their iWUE in response to rising daily temperatures for both earlywood and latewood. High vapor

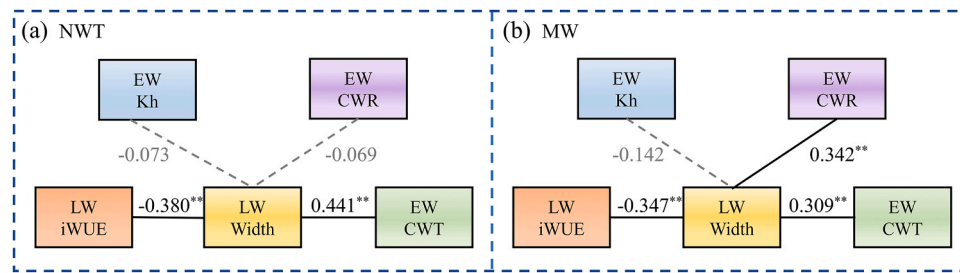


Fig. 7. Relationships between anatomical indicators and iWUE and tree-ring width reflected by Pearson's correlation coefficients. Dark solid lines indicate significant relationships, grey dotted lines indicate insignificant relationships. **, $P < 0.01$. EW indicates earlywood and LW indicates latewood.

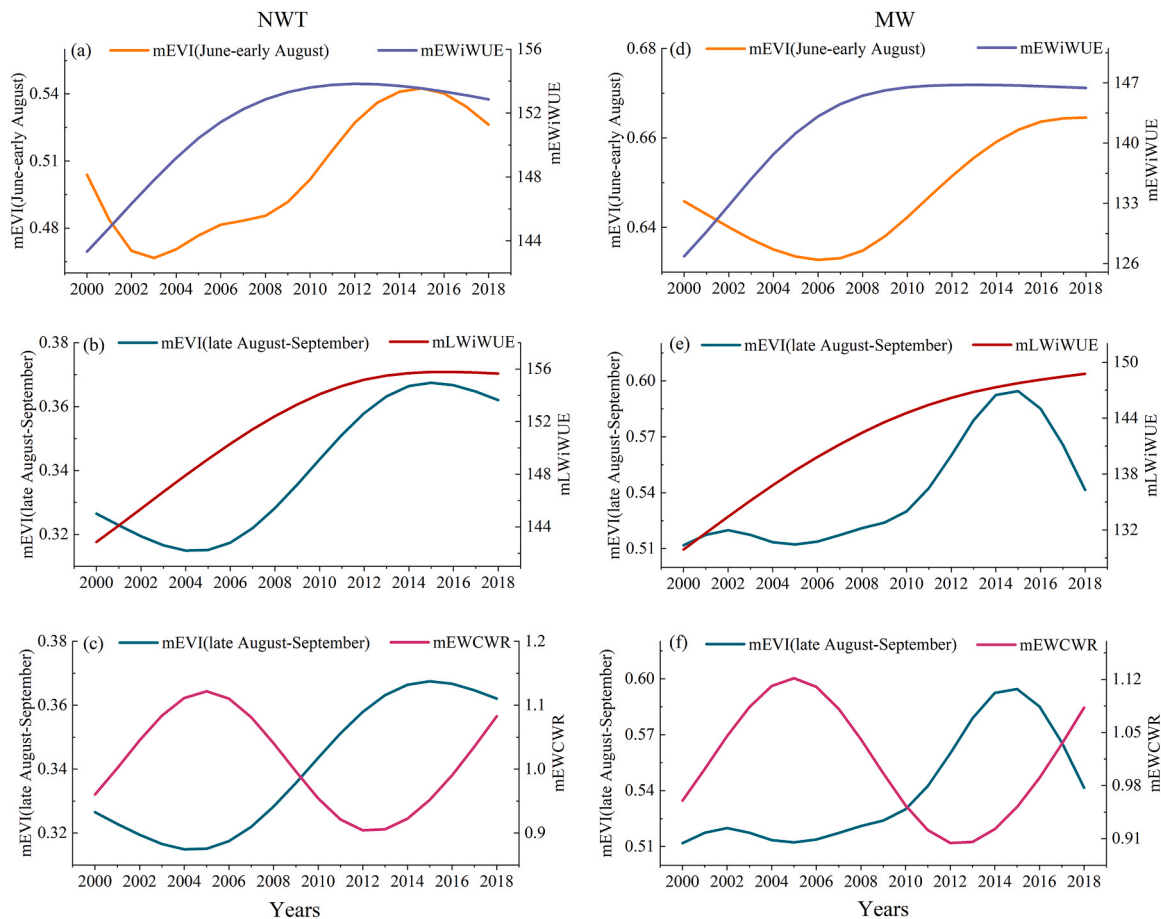


Fig. 8. Relationships between iWUE and EVI and those between CWR and EVI reflected by generalized additive model at NWT (a-c) and MW (d-f). EW indicates earlywood and LW indicates latewood.

pressure deficits from elevated temperatures are known to increase trees' intrinsic iWUE, as previously observed in temperate (Li et al., 2023) and mediterranean woodlands (Olano et al., 2014). Although lower precipitation (June-July) was also related to higher latewood iWUE on the drier slope, only a mild negative association was noted with precipitation (May) for earlywood at the wetter slope. Indeed, negative iWUE anomalies under extremely low precipitation on the wetter slope suggest a complex response of $\delta^{13}\text{C}$ to precipitation, which could be related to isotope signal blurring effects caused by post-assimilation processes (Cernusak, 2020), such as storage. According to the xylogenesis data of *P. tabuliformis* at NWT (data not published yet), latewood would be formed after late August, which suggests that the latewood $\delta^{13}\text{C}$ is mainly influenced by conditions from months prior to its formation. Moreover, we found strong deviations from average iWUE in earlywood following extremely dry and wet years, especially on the

wetter slope. These results could be attributed to a large reliance of $\delta^{13}\text{C}$ on stored carbon. A similar study about *P. pinea* also suggested that earlywood was likely formed using both recently and formerly assimilated carbon, while latewood relied mostly on carbon accumulated many months prior to its formation (Castagneri et al., 2018). A large reliance of $\delta^{13}\text{C}$ on stored carbon is also in line with the results reported in a previous study in *Larix gmelinii* using pulse-labelling $^{13}\text{C}\text{O}_2$ in photoassimilates (Kagawa et al., 2006). From another aspect, abnormally low iWUE on the wetter slope in the extremely dry year could also be driven by impaired photosynthetic performance due to drought-induced biochemical damage of the leaf photosynthetic machinery (Zhu et al., 2023).

5. iWUE modulates the anatomical response of trees to precipitation similarly on contrasting moisture-level slopes

The dynamic responses of anatomical structures to precipitation were significantly modulated by increasing iWUE. On the drier slope, the negative responses of Kh and the positive responses of CWR to mid-summer precipitation strengthened along with increasing iWUE. On the wetter slope, the positive responses of Kh and the negative responses of CWR to precipitation in late growing season also strengthened with rising iWUE. Taken together, these results suggest that warming-induced increments in iWUE intensified the sensitivity of xylem anatomy adjustments to water availability. Such phenomenon mainly occurred when iWUE was $< 145 \mu\text{mol mol}^{-1}$, whereas iWUE values $> 145 \mu\text{mol mol}^{-1}$ weakened the climate sensitivity of hydraulic efficiency and safety indicators, which was only a small part of the overall trend. Thus, iWUE appears to regulate the responses of anatomical indicators to climate consistently across various environmental conditions. This phenomenon has been attributed to the possible influence of recently assimilated carbon availability on xylem formation (Galiano et al., 2011; Olano et al., 2014). However, covariation between climate responses of iWUE and xylem anatomy cannot be ruled out. In addition to causing stomatal closure, severe summer drought on the drier slope could limit pine's ability to invest in thick-walled tracheids by impairing leaf photosynthetic functions or restricting cambial activity and cell wall deposition (Fernandez-de-Una et al., 2017). Conversely, autumn conditions increasing iWUE on the wetter slope may be mild enough to allow an extension of tracheid differentiation periods, which is characteristically long and sensitive to climate in latewood tracheids (Cuny et al., 2014).

Previous studies have primarily focused on the dynamic response of tree anatomy to climate change (Islam et al., 2018). For example, studies in tropical moist forests show that increasing late-winter temperatures can alter the length of the growing season and the sensitivity of tree-ring variables in *Toona ciliata* M. Roem (Islam et al., 2019). However, investigations into the influence of iWUE on the climate sensitivity of wood anatomy are still limited. Therefore, we believe our study shed light on the dynamic interplay among xylem anatomy, iWUE, and climate in temperate conifers.

6. Similar associations of anatomical indicators and iWUE with tree-ring width and EVI across moisture-level slopes

Pearson's correlation analysis revealed the correspondence between earlywood anatomical structure and latewood width across different slopes at a high-frequency scale. On the wetter slope (MW), latewood width was positively related to CWR and CWT of earlywood, while on the drier slope (NWT) we only found a positive association between latewood width and earlywood CWT. This result suggests that earlywood anatomy traits affect latewood formation, with enhanced hydraulic safety in earlywood favoring latewood cell production. This idea would be supported by the strong developmental connections between tracheid morphology and cell production found in temperate and boreal conifers (Hong et al., 2021; Saiki and Kawake, 1980). In turn, the lack of correspondence between CWR and latewood width on the drier slope may be explained by the stronger environmental control of radial growth during latewood formation at this slope, which could mask possible functional effects from earlywood cell lumen size.

Our analysis also revealed a negative association between latewood iWUE and latewood width at both slopes, which is in accordance with their opposite responses to warming. This result is consistent with previous studies suggesting that stringent stomatal control is related to limited tree-ring width (Rodríguez-Caton et al., 2021). iWUE, determined by the balance between photosynthesis (A) and stomatal conductance to water vapor (g_s), generally increases with high A and/or low g_s (Cernusak, 2020). Trees modulate stomatal apertures in response to environmental moisture deficits, with g_s being relatively low under

high moisture stress, thus influencing iWUE (Cowan and Farquhar, 1977). Thus, our study pines largely coped with water deficits by reducing g_s , which limited transpiration and increased the $\delta^{13}\text{C}$ signature of sugars used in tracheid wall construction. At the same time, water stress may have limited cell division and enlargement in the stem, partly as a consequence of a decreasing cell turgor (Cosgrove, 2005; Hölttä et al., 2010). These findings corroborate the idea that *P. tabuliformis* may prioritize carbon storage over radial growth during periods of low assimilation.

Considering multiyear low-frequency dynamics, our study revealed that xylem anatomy significantly influenced canopy dynamics, as reflected by the EVI—a proxy for aboveground net primary production (Cabello et al., 2012). It was also noted that both iWUE and EVI increased with a lag from 2003 to 2015. Although iWUE and EVI could increase with tree age (Köhl et al., 2017), in this study, most trees are over 100 years old and belong to mature forests (Fig. S7), so the impact of age on these two indicators is minimal. Over the long term, while $\delta^{13}\text{C}$ has shown significant low-frequency fluctuations over the past 60 years, iWUE has consistently increased (Fig. S8), likely due to rising atmospheric CO_2 levels (Mathias and Thomas, 2021). Higher CO_2 enhances tree photosynthesis, promoting canopy growth. However, canopy growth also depends on water availability. Between 2003 and 2015, an upward trend in the P-PET of growing season facilitated canopy growth and increased EVI. Conversely, when the P-PET of growing season declined, EVI tended to decrease with a lag (Fig. S2). The above reasons lead to synchronous uptrend between iWUE and EVI during 2003–2015.

On the other hand, high earlywood CWR values were associated with lower EVI values from late August to September on both slopes, which was apparently driven by an inverse relationship between EVI and CWT. We hypothesize that increased biomass allocation to earlywood formation (high earlywood CWR) could negatively affect the tree's carbon balance, which may somewhat hamper canopy processes if unfavorable moist conditions trigger stomatal closure in summer. In addition, lower hydraulic efficiency may limit photosynthesis in trees showing high CWR (Boyer, 1976). However, this association was reversed at the drier slopes during latewood formation, with both latewood CWT and EVI showing positive trends. This suggests that enhanced assimilation in summer would help minimize the observed drought-induced decline in carbon sequestration into the tree-ring structure.

This study has certain limitations that pertain to the precise determination of the timing and location of xylem formation responsible for water transport to the canopy. The exact mechanisms through which iWUE influences anatomical responses to climate and canopy dynamics remain unclear. The exact temporal and spatial resolution of xylem development remains elusive, which consequently obscures the specific mechanisms by which the anatomical structure influences canopy dynamics. This limitation underscores the need for further in-depth research employing more refined methodologies that can offer higher resolution in tracking xylem formation and canopy dynamics.

7. Conclusion

Retrospective analysis, which integrates xylem anatomical and carbon stable isotope indices, provides insights into the adaptive strategies of *Pinus tabuliformis* to cope with climate change in China. The findings reveal that trees on drier slopes adopt an acquisitive strategy, characterized by increased hydraulic efficiency to prioritize carbon assimilation and storage over allocation to growth. Conversely, trees on wetter slopes, a conservative hydraulic strategy that increases hydraulic safety and woody biomass. These adaptations are further complemented by increasing iWUE, which strengthened the climate sensitivity of hydraulic efficiency and safety indicators. Integrating canopy dynamics with radial growth data reveals that adjustments in xylem structure and physiological strategies affect carbon assimilation, storage, and allocation. These findings are essential for predicting future forest dynamics and the capacity of forests to sequester carbon, which has implications

for climate change mitigation and adaptation strategies.

CRedit authorship contribution statement

Gonzalo Pérez-de-Lis: Writing – review & editing. **Yan Liu:** Visualization. **Yixue Hong:** Methodology, Investigation. **Lingnan Zhang:** Writing – original draft, Methodology, Funding acquisition, Formal analysis. **Xiaohong Liu:** Funding acquisition, Conceptualization. **Yan-jun Song:** Writing – review & editing. **Xiaomin Zeng:** Validation.

Declaration of Competing Interest

The authors declare that they have no known competing financial interests or personal relationships that could have appeared to influence the work reported in this paper.

Acknowledgements

This work was supported by the National Natural Science Foundation of China (42330501 and 42171055) and the Fundamental Research Funds for the Central Universities (GK202309010). GPL benefited from the *Xunta de Galicia* grants (ED481D 2023/012 and ED431C 2023/19).

Appendix A. Supporting information

Supplementary data associated with this article can be found in the online version at [doi:10.1016/j.envexpbot.2025.106087](https://doi.org/10.1016/j.envexpbot.2025.106087).

Data availability statement

Data available from the Dryad Digital Repository (<http://datadryad.org/stash/share/YoFkXAIb1enQEMBXrhMQWVUVVvDQC9sImbYrYFT8X08>).

References

- Allen, C.D., Macalady, A.K., Chenchouni, H., Bachelet, D., McDowell, N., Vennetier, M., Kitzberger, T., Rigling, A., Breshears, D.D., Hogg, E.T., 2010. A global overview of drought and heat-induced tree mortality reveals emerging climate change risks for forests. *For. Ecol. Manag.* 259, 660–684. <https://doi.org/10.1016/j.foreco.2009.09.001>.
- Arguelles-Marron, B., Meave, J.A., Luna-Vega, I., Crispin-DelaCruz, D.B., Szejner, P., Ames-Martinez, F.N., Rodriguez-Ramirez, E.C., 2023. Adaptation potential of Neotropical montane oaks to drought events: Wood anatomy sensitivity in *Quercus delgadoana* and *Quercus meavei*. *Funct. Ecol.* 37, 2040–2055. <https://doi.org/10.1111/1365-2435.14362>.
- Ault, T.R., 2020. On the essentials of drought in a changing climate. *Science* 368, 256–260. <https://doi.org/10.1126/science.aaz5492>.
- Babst, F., Bouriaud, O., Poulter, B., Trouet, V., Girardin, M.P., Frank, D.C., 2019. Twentieth century redistribution in climatic drivers of global tree growth. *Sci. Adv.* 5. <https://doi.org/10.1126/sciadv.aat4313>.
- Boyer, J., 1976. Water deficits and photosynthesis. In: Kozlowski, T.T. (Ed.), *Water deficits and plant growth*. Academic Press, pp. 153–190.
- Brodribb, T.J., McAdam, S.A.M., 2017. Evolution of the stomatal regulation of plant water content. *Plant Physiol.* 174, 639–649. <https://doi.org/10.1104/pp.17.00078>.
- Brodribb, T.J., Powers, J., Cochar, H., Choat, B., 2020. Hanging by a thread? Forests and drought. *Science* 368, 261–266. <https://doi.org/10.1126/science.aat7631>.
- Bunn, A.G., 2008. A dendrochronology program library in R (dplR). *Dendrochronologia* 26, 115–124. <https://doi.org/10.1016/j.dendro.2008.01.002>.
- Cabello, J., Alcaraz-Segura, D., Ferrero, R., Castro, A.J., Liras, E., 2012. The role of vegetation and lithology in the spatial and inter-annual response of EVI to climate in drylands of Southeastern Spain. *J. Arid. Environ.* 79, 76–83. <https://doi.org/10.1016/j.jaridenv.2011.12.006>.
- Castagneri, D., Battipaglia, G., von Arx, G., Pacheco, A., Carrer, M., 2018. Tree-ring anatomy and carbon isotope ratio show both direct and legacy effects of climate on bimodal xylem formation in *Pinus pinea*. *Tree Physiol.* 38, 1098–1109. <https://doi.org/10.1093/treephys/tpy036>.
- Cernusak, L.A., 2020. Gas exchange and water-use efficiency in plant canopies. *Plant Biol.* 22, 52–67. <https://doi.org/10.1111/plb.12939>.
- Chen, Z., Zhang, Y., Li, Z., Han, S., Wang, X., 2022. Climate change increased the intrinsic water use efficiency of *Larix gmelinii* in permafrost degradation areas, but did not promote its growth. *Agric. For. Meteorol.* 320, 108957. <https://doi.org/10.1016/j.agrformet.2022.108957>.
- Cosgrove, D.J., 2005. Growth of the plant cell wall. *Nat. Rev. Mol. Cell Biol.* 6, 850–861. <https://doi.org/10.1038/nrm1746>.
- Cowan, I.R., Farquhar, G.D., 1977. Stomatal function in relation to leaf metabolism and environment. *Symp. Soc. Exp. Biol.* 31, 471–505. [https://doi.org/10.1016/S0081-3021\(08\)60105-0](https://doi.org/10.1016/S0081-3021(08)60105-0).
- Denne, M., 1989. Definition of latewood according to Mork (1928). *IAWA J.* 10, 59–62. <https://doi.org/10.1163/22941932-90001112>.
- Eilmann, B., Zweifel, R., Buchmann, N., Fonti, P., Rigling, A., 2009. Drought-induced adaptation of the xylem in Scots pine and pubescent oak. *Tree Physiol.* 29, 1011–1020. <https://doi.org/10.1093/treephys/tpp035>.
- Fernandez-de-Una, L., Rossi, S., Aranda, I., Fonti, P., Gonzalez-Gonzalez, B.D., Canellas, I., Gea-Izquierdo, G., 2017. Xylem and leaf functional adjustments to drought in *Pinus sylvestris* and *Quercus pyrenaica* at their elevational boundary. *Front. Plant Sci.* 8. <https://doi.org/10.3389/fpls.2017.01200>.
- Galiano, L., Martínez-Vilalta, J., Lloret, F., 2011. Carbon reserves and canopy defoliation determine the recovery of Scots pine 4 yr after a drought episode. *N. Phytol.* 190, 750–759. <https://doi.org/10.1111/j.1469-8137.2010.03628.x>.
- González de Andrés, E., Suárez, M.L., Querejeta, J.I., Camarero, J.J., 2021. Chronically low nutrient concentrations in tree rings are linked to greater tree vulnerability to drought in *Nothofagus dombeyi*. *Forests* 12, 1180. <https://doi.org/10.3390/f12091180>.
- González-M, R., Posada, J.M., Carmona, C.P., Garzón, F., Salinas, V., Idárraga-Piedrahita, Á., Pizano, C., Avella, A., López-Camacho, R., Norden, N., 2021. Diverging functional strategies but high sensitivity to an extreme drought in tropical dry forests. *Ecol. Lett.* 24, 451–463. <https://doi.org/10.1111/ele.13659>.
- Granda, E., Rossatto, D.R., Camarero, J.J., Voltas, J., Valladares, F., 2014. Growth and carbon isotopes of Mediterranean trees reveal contrasting responses to increased carbon dioxide and drought. *Oecologia* 174, 307–317. <https://doi.org/10.1007/s00442-013-2742-4>.
- Hacke, U.G., Sperry, J.S., Pockman, W.T., Davis, S.D., McCulloh, K.A., 2001. Trends in wood density and structure are linked to prevention of xylem implosion by negative pressure. *Oecologia* 126, 457–461. <https://doi.org/10.1007/s004420100628>.
- Han, R., Gong, X., Li, M., Leng, Q., Zhou, Y., Ning, Q., Hao, G., 2023. Combined tree-ring width and wood anatomy chronologies provide insights into the radial growth and hydraulic strategies in response to an extreme drought in plantation-grown Mongolian pine trees. *Environ. Exp. Bot.* 208, 105259. <https://doi.org/10.1016/j.envexpbot.2023.105259>.
- Holmes, R.L., 1983. Computer-assisted quality control in tree-ring dating and measurement. *Tree-Ring Bull.* 43, 69–78.
- Hölttä, T., Mäkinen, H., Nöjd, P., Mäkelä, A., Nikinmaa, E., 2010. A physiological model of softwood cambial growth. *Tree Physiol.* 30, 1235–1252. <https://doi.org/10.1093/treephys/tpq068>.
- Hong, Y., Zhang, L., Liu, X., Aritsara, A.N.A., Zeng, X., Xing, X., Lu, Q., Wang, K., Wang, Y., Zhang, Y., Wang, W., 2021. Tree ring anatomy indices of *Pinus tabulaeformis* revealed the shifted dominant climate factor influencing potential hydraulic function in western Qinling Mountains. *Dendrochronologia* 70, 125881. <https://doi.org/10.1016/j.dendro.2021.125881>.
- IPCC, 2021. Summary for Policymakers. *Climate Change 2021: The physical science Basis. Contribution of working group I to the sixth assessment report of the intergovernmental panel on climate change*. Cambridge University Press, Cambridge.
- Islam, M., Rahman, M., Bräuning, A., 2018. Xylem anatomical responses of diffuse porous *Chukrasia tabularis* to climate in a South Asian moist tropical forest. *For. Ecol. Manag.* 412, 9–20. <https://doi.org/10.1016/j.foreco.2018.01.035>.
- Islam, M., Rahman, M., Bräuning, A., 2019. Long-term wood anatomical time series of two ecologically contrasting tropical tree species reveal differential hydraulic adjustment to climatic stress. *Agric. For. Meteorol.* 265, 412–423. <https://doi.org/10.1016/j.agrformet.2018.11.037>.
- Jia, H.S., Guan, C.F., Zhang, J.S., He, C.X., Yin, C.J., Meng, P., 2022. Drought effects on tree growth, water use efficiency, vulnerability and canopy health of *Quercus variabilis-Robinia pseudoacacia* mixed plantation. *Front. Plant Sci.* 13. <https://doi.org/10.3389/fpls.2022.1018405>.
- Kagawa, A., Sugimoto, A., Maximov, T.C., 2006. ¹³C₂ pulse-labelling of photoassimilates reveals carbon allocation within and between tree rings. *Plant Cell Environ.* 29, 1571–1584. <https://doi.org/10.1111/j.1365-3040.2006.01491.x>.
- Köhl, M., Neupane, P.R., Lotfiomran, N., 2017. The impact of tree age on biomass growth and carbon accumulation capacity: A retrospective analysis using tree ring data of three tropical tree species grown in natural forests of Suriname. *PLoS One* 12, e0181187. <https://doi.org/10.1371/journal.pone.0181187>.
- Lachenbruch, B., McCulloh, K.A., 2014. Traits, properties, and performance: how woody plants combine hydraulic and mechanical functions in a cell, tissue, or whole plant. *N. Phytol.* 204, 747–764. <https://doi.org/10.1111/nph.16973>.
- Lange, J., Carrer, M., Pisarcic, M.F., Porter, T.J., Seo, J.W., Trouillier, M., Wilmking, M., 2020. Moisture-driven shift in the climate sensitivity of white spruce xylem anatomical traits is coupled to large-scale oscillation patterns across northern treeline in northwest North America. *Glob. Change Biol.* 26, 1842–1856. <https://doi.org/10.1111/gcb.14947>.
- Li, Y., Xu, C., Huang, Y., Huo, X., Shi, F., Pan, Y., Ren, L., Wu, X., 2023. Tree growth and intrinsic water use efficiency of Chinese pine plantations along a precipitation gradient in northern China. *For. Ecol. Manag.* 528, 120609. <https://doi.org/10.1016/j.foreco.2022.120609>.
- Liang, W., Heinrich, I., Simard, S., Helle, G., Liñán, I.D., Heinken, T., 2013. Climate signals derived from cell anatomy of Scots pine in NE Germany. *Tree Physiol.* 33, 833–844. <https://doi.org/10.1093/treephys/tp059>.
- Liang, X., He, P., Liu, H., Zhu, S., Uyehara, I.K., Hou, H., Wu, G., Zhang, H., You, Z., Xiao, Y., Ye, Q., 2019. Precipitation has dominant influences on the variation of plant hydraulics of the native *Castanopsis fargesii* (Fagaceae) in subtropical China.

- Agric. For. Meteorol. 271, 83–91. <https://doi.org/10.1016/j.agrformet.2019.02.043>.
- Linares, J.C., Camarero, J.J., 2011. From pattern to process: linking intrinsic water-use efficiency to drought-induced forest decline. *Glob. Change Biol.* 18, 1000–1015. <https://doi.org/10.1111/j.1365-2486.2011.02566.x>.
- Martin-Benito, D., Anchukaitis, K.J., Evans, M.N., Del Río, M., Beekman, H., Cañellas, I., 2017. Effects of drought on xylem anatomy and water-use efficiency of two co-occurring pine species. *Forests* 8, 332. <https://doi.org/10.3390/f8090332>.
- Mathias, J.M., Thomas, R.B., 2021. Global tree intrinsic water use efficiency is enhanced by increased atmospheric CO₂ and modulated by climate and plant functional types. *Proc. Natl. Acad. Sci. USA* 118, e2014286118. <https://doi.org/10.1073/pnas.2014286118>.
- Olano, J.M., Linares, J.C., García-Cervigón, A.I., Arzac, A., Delgado, A., Rozas, V., 2014. Drought-induced increase in water-use efficiency reduces secondary tree growth and tracheid wall thickness in a Mediterranean conifer. *Oecologia* 176, 273–283. <https://doi.org/10.1007/s00442-014-2989-4>.
- Peñuelas, J., Canadell, J.G., Ogaya, R., 2011. Increased water-use efficiency during the 20th century did not translate into enhanced tree growth. *Glob. Ecol. Biogeogr.* 20, 597–608.
- Pfautsch, S., Harbusch, M., Wesolowski, A., Smith, R., Macfarlane, C., Tjoelker, M.G., Reich, P.B., Adams, M.A., 2016. Climate determines vascular traits in the ecologically diverse genus *Eucalyptus*. *Ecol. Lett.* 19, 240–248. <https://doi.org/10.1111/ele.12559>.
- Piper, F.I., Fajardo, A., Hoch, G., 2017. Single-provenance mature conifers show higher non-structural carbohydrate storage and reduced growth in a drier location. *Tree Physiol.* 37, 1001–1010. <https://doi.org/10.1093/treephys/tpx061>.
- Puchi, P.F., Camarero, J.J., Battipaglia, G., Carrer, M., 2021. Retrospective analysis of wood anatomical traits and tree-ring isotopes suggests site-specific mechanisms triggering *Araucaria araucana* drought-induced dieback. *Glob. Change Biol.* 27, 6394–6408. <https://doi.org/10.1111/gcb.15881>.
- Rodriguez-Caton, M., Andreu-Hayles, L., Morales, M.S., Daux, V., Christie, D.A., Coopman, R.E., Alvarez, C., Rao, M.P., Aliste, D., Flores, F., 2021. Different climate sensitivity for radial growth, but uniform for tree-ring stable isotopes along an aridity gradient in *Polylepis tarapacana*, the world's highest elevation tree species. *Tree Physiol.* 41, 1353–1371. <https://doi.org/10.1093/treephys/tpab021>.
- Růžička, K., Ursache, R., Hejálko, J., Helariutta, Y., 2015. Xylem development—from the cradle to the grave. *N. Phytol.* 207, 519–535. <https://doi.org/10.1111/nph.13383>.
- Saiki, H., Kawake, M., 1980. Structure of starved wood in *Akamatsu* (*Pinus densiflora* Sieb. et Zucc.). *Mokuzai Gakkaishi* 26, 707–713.
- Saurer, M., Voelker, S., 2022. Intrinsic water-use efficiency derived from stable carbon isotopes of tree-rings. In: *Stable Isotopes in Tree Rings*. Springer International Publishing, Cham, pp. 481–498.
- Saurer, M., Siegwolf, R.T., Schweingruber, F.H., 2004. Carbon isotope discrimination indicates improving water-use efficiency of trees in northern Eurasia over the last 100 years. *Glob. Change Biol.* 10, 2109–2120. <https://doi.org/10.1111/j.1365-2486.2004.00869.x>.
- Schuldt, B., Knutzen, F., Delzon, S., Jansen, S., Müller-Haubold, H., Burrell, R., Clough, Y., Leuschner, C., 2016. How adaptable is the hydraulic system of European beech in the face of climate change-related precipitation reduction? *N. Phytol.* 210, 443–458. <https://doi.org/10.1111/nph.13798>.
- Shi, H., Peng, X., Zhou, Y.-J., Wang, A.-Y., Sun, X.-K., Li, N., Bao, Q.-S., Buri, G., Hao, G.-Y., 2024. Resilience and response: Unveiling the impacts of extreme droughts on forests through integrated dendrochronological and remote sensing analyses. *For. Ecosyst.* 11, 100209. <https://doi.org/10.1016/j.fecs.2024.100209>.
- Song, W., Zhao, B., Mu, C., Ballikaya, P., Cherubini, P., Wang, X., 2022. Moisture availability influences the formation and characteristics of earlywood of *Pinus tabuliformis* more than latewood in northern China. *Agric. For. Meteorol.* 327, 109219. <https://doi.org/10.1016/j.agrformet.2022.109219>.
- Song, Y., Poorter, L., Horsting, A., Delzon, S., Sterck, F., 2021. Pit and tracheid anatomy explain hydraulic safety but not hydraulic efficiency of 28 conifer species. *J. Exp. Bot.* 73, 1033–1048. <https://doi.org/10.1093/jxb/erab449>.
- Sperry, J.S., Venturas, M.D., Anderegg, W.R.L., Mencuccini, M., Mackay, D.S., Wang, Y., Love, D.M., 2017. Predicting stomatal responses to the environment from the optimization of photosynthetic gain and hydraulic cost. *Plant Cell Environ.* 40, 816–830. <https://doi.org/10.1111/pce.12852>.
- Tyree, M.T., Dixon, M.A., 1986. Water stress induced cavitation and embolism in some woody plants. *Physiol. Plant.* 66, 397–405. <https://doi.org/10.1111/j.1399-3054.1986.tb05941.x>.
- Wang, L., Chen, W., 2014. A CMIP5 multimodel projection of future temperature, precipitation, and climatological drought in China. *Int. J. Climatol.* 34, 2059–2078. <https://doi.org/10.1002/joc.3822>.
- Wang, W., Liu, X., An, W., Xu, G., Zeng, X., 2012. Increased intrinsic water-use efficiency during a period with persistent decreased tree radial growth in northwestern China: Causes and implications. *For. Ecol. Manag.* 275, 14–22. <https://doi.org/10.1016/j.foreco.2012.02.027>.
- Zhang, J., Bai, H., Yuan, B., Ma, X., 2013. Statistical downscaling of air temperature change in the Qinling mountains. *Arid Zone Res* 30, 322–328. <https://doi.org/10.13866/j.azr.2013.02.023>.
- Zhang, Y., Qin, Q., Zhu, Q., Sun, X., Bai, Y., Liu, Y., 2023. Stable isotopes in tree rings record physiological trends in *Larix gmelinii* after fires. *Tree Physiol.* 43, 1066–1080. <https://doi.org/10.1093/treephys/tpad033>.
- Zhu, R., Hu, T., Wu, F., Liu, Y., Zhou, S., Wang, Y., 2023. Photosynthetic and hydraulic changes caused by water deficit and flooding stress increase rice's intrinsic water-use efficiency. *Agr. Water Manag.* 289, 108527. <https://doi.org/10.1016/j.agwat.2023.108527>.
- Zuidema, P.A., Heinrich, I., Rahman, M., Vlam, M., Zwartsenberg, S.A., van der Sleen, P., 2020. Recent CO₂ rise has modified the sensitivity of tropical tree growth to rainfall and temperature. *Glob. Change Biol.* 26, 4028–4041. <https://doi.org/10.1111/gcb.15092>.